Korean J. Chem. Eng., 39(11), 2925-2934 (2022)
DOI: 10.1007/s11814-022-1235-8

pISSN: 0256-1115
eISSN: 1975-7220

Techno-economic analysis of the integrated DME production process: Effects of different separation trains and recycling strategies

Hyeon Park*, Jong Wook Bae, Gookhee Kim***,†, and Myung-June Park*,****,†**

*Department of Energy Systems Research, Ajou University, Suwon 16499, Korea
**School of Chemical Engineering, Sungkyunkwan University (SKKU), Suwon 16419, Korea
***Research Institute of Industrial Science & Technology (RIST), Pohang 37673, Korea
****Department of Chemical Engineering, Ajou University, Suwon 16499, Korea
(*Received 19 April 2022 • Revised 29 June 2022 • Accepted 19 July 2022*)

Abstract−Integrated process models were developed to produce dimethyl ether (DME) from the byproduct gas of the steelmaking process. Two different separation trains (the use of flash drums to separate light gases followed by two columns to separate CO_2 and DME vs. the application of an absorber to separate light gas and CO_2 under mild temperatures), and two different recycling strategies (recycling with and without further separation of hydrogen by a membrane) were considered. Detailed kinetic reactions for methanol (MeOH) synthesis from syngas and the dehydration of MeOH to DME were used in the reactor model, which helped predict the compositions of the reactor effluent under various conditions and determine the operating conditions of the separation trains. Both separation trains with recycled stream increased the DME production rate and overall CO_2 conversion, while the sizes of the reactor and separators, and the utility costs of refrigeration, absorbent recovery, recycled stream compression, etc. were significantly increased. The tradeoffs between different cases were quantitatively analyzed by techno-economic and sensitivity analyses. The results showed that the use of the absorber with the recycling of hydrogen is the most feasible process for the economic production of DME with high CO_2 reduction.

Keywords: Dimethyl Ether, Detailed Kinetic Rates, Separation Trains, Recycling, Techno-economic Analysis, CO_2 Reduction

INTRODUCTION

Dimethyl ether (DME) is a potential intermediate to replace conventional diesel and liquified petroleum gas because of its high cetane number and low self-ignition temperature [1]. It is also regarded as a clean energy source for next-generation fuels because its combustion does not generate harmful components such as NO_x, smoke, and particulates [2].

DME can be produced from syngas using two different methods. The first is a two-step process in which methanol (MeOH) is synthesized in the first reactor followed by dehydration in the next reactor. The second is a single-step process in which MeOH synthesis and dehydration occur simultaneously in a single reactor. A comparison of the two methods has shown that CO and CO_2 conversion, DME selectivity, and DME yield in the single-step process were higher than those in the two-step process [3,4].

Despite the advantages of the single-step method in terms of conversion and yield, its separation process for high-purity DME is relatively more complex because of the presence of additional components in the reactor effluent [5]. Nevertheless, it has attracted attention because of its thermodynamic advantages and higher DME productivity [6].

A few DME synthesis processes based on a single-step reactor using syngas from various sources have been proposed to improve economic feasibility and reduce CO_2 emissions. The Korea Gas Corporation has launched a 10 tons per day (TPD) demo plant for single-step DME synthesis with tri-reforming and established the basic design of a commercial plant that can produce 3,000 TPD of DME [7]. A rigorous single-step process to produce DME from syngas by tri-reforming has been proposed to maximize CO_2 conversion [8]. Clausen et al. conducted a techno-economic assessment of a single-step DME synthesis plant based on the gasification of torrefied wood pellets and analyzed CO_2 emission. They found that the cost of DME production using the proposed process was 12.9 \$/GJ_{LHV} (LHV: lower heating value), while CO_2 emission decreased by approximately 10% [9]. Mevawala et al. performed a techno-economic analysis of the shale gas to DME process using the Aspen Process Economic Analyzer based on the rigorous process model developed in Aspen Plus® (Aspen Technology, Inc.). The effects of key design parameters (e.g., H_2/CO in the syngas) and investment parameters (e.g., plant scale, raw material costs, products, and utilities) on the process economics were evaluated [10].

However, most of the reported works on the single-step DME synthesis process are based on the experimental data, not on the detailed reaction kinetics, and the effects of the different separation strategies on the techno-economics of the processes have rarely been evaluated. Therefore, in this study, a techno-economic assessment for quantitative comparisons between different separation cases was conducted to determine the appropriate and economically feasible integrated DME synthesis process. A single-step DME synthesis pro-

†To whom correspondence should be addressed.
E-mail: gookheekim@rist.re.kr, mjpark@ajou.ac.kr

cess using byproduct gas from the steelmaking process was considered. To obtain high-purity DME, two different separation schemes were applied: flash separation to separate unconverted syngas followed by the separation of CO_2 and DME, and the use of an absorber to separate light gas and CO_2. For each separation train, two different strategies for the recycled stream were considered. One is the recycling of unreacted gas, CO_2, and inert gas. The other is the separation of hydrogen using a membrane and its recycling to the reactor. Because different separation trains and recycling strategies lead to different compositions at the reactor inlet, detailed kinetic rate equations were considered to predict the compositions of the reactor effluent and determine the operating conditions of the separation trains.

METHODS

1. Reaction Rates and Reactor Modeling

In our previous work [4], we developed kinetic rate equations for the synthesis of DME from syngas over physically mixed Cu-ZnO-Al_2O_3 (CZA; MeOH synthesis from syngas) and ferrierite (FER; MeOH dehydration to DME) catalysts. The overall reaction mechanism for MeOH synthesis consists of three reactions: CO and CO_2 hydrogenation and the water-gas shift (WGS) reaction [11]. The mechanism for the dehydration of MeOH reported in the literature [12] was used in the present study.

CO hydrogenation: $CO\ (g)+2H_2\ (g)\rightleftarrows CH_3OH\ (g)$ (1)

CO_2 hydrogenation: $CO_2\ (g)+3H_2\ (g)\rightleftarrows CH_3OH\ (g)+H_2O\ (g)$ (2)

Water-gas shift (WGS): $CO\ (g)+H_2O\ (g)\rightleftarrows CO_2\ (g)+H_2\ (g)$ (3)

MeOH dehydration: $2CH_3OH\ (g)\rightleftarrows CH_3OCH_3\ (g)+H_2O\ (g)$ (4)

The physical mixing of the two catalysts in a single reactor has advantages over the two reactors (one each for MeOH and DME syntheses). In the case of two reactors, the CO and CO_2 conversions in the first reactor were restricted by the equilibrium (equilibrium conversions of approximately 40% and 15% for CO and CO_2 hydrogenation, respectively, under the reference conditions of 250 °C, 5 MPa, and a space velocity of 5,000 L/(kg_{cat}·h), resulting in a very low DME production rate despite a high MeOH dehydration rate. In contrast, the direct synthesis of DME from syngas in a single reactor by physically mixing the CZA and FER catalysts had equilibrium conversions of approximately 100% and a maximum of 50% for CO and CO_2 hydrogenation, respectively. The reason was that the MeOH produced was instantaneously converted to DME, thus reducing the reverse reaction rate. The present study adopted the same specifications for the single reactor (physical mixing of CZA and FER catalysts with the volumetric ratio of the CZA to FER set as 10).

Note that reactor models with detailed kinetic rate equations were used in the present study because the different process configurations, such as the introduction of the recycled stream, result in different compositions of the reactor effluent, which in turn influences the operating conditions of the separation trains in the entire process. Therefore, the reaction rates and kinetic parameters estimated in our previous work [4] were used without modification because the same catalysts with the same volumetric ratio were considered. The operating windows were also assumed to be the same.

CO hydrogenation:

$$r_{CO}=\frac{k_{CO}K_{CO}^{ad}[f_{CO}f_{H_2}^{1.5}-f_{MeOH}/(K_{P,1}f_{H_2}^{0.5})]}{(1+K_{CO}^{ad}f_{CO})(1+\sqrt{K_{H_2}^{ad}f_{H_2}}+K_{H_2O}^{ad}f_{H_2O})} \quad (5)$$

CO_2 hydrogenation:

$$r_{CO_2}=\frac{k_{CO_2}K_{CO_2}^{ad}[f_{CO_2}f_{H_2}^{1.5}-f_{H_2O}f_{MeOH}/(K_{P,3}f_{H_2}^{1.5})]}{(1+K_{CO_2}^{ad}f_{CO_2})(1+\sqrt{K_{H_2}^{ad}f_{H_2}}+K_{H_2O}^{ad}f_{H_2O})} \quad (6)$$

Water-gas shift (WGS):

$$r_{WGS}=-\frac{k_{WGS}K_{CO_2}^{ad}[f_{CO_2}f_{H_2}-f_{CO}f_{H_2O}/K_{P,2}]}{(1+K_{CO_2}^{ad}f_{CO_2})(1+\sqrt{K_{H_2}^{ad}f_{H_2}}+K_{H_2O}^{ad}f_{H_2O})} \quad (7)$$

MeOH dehydration:

$$r_{DME}=\frac{k_{DME}(K_{MeOH}^{ad})^2[C_{MeOH}^2-(C_{H_2O}C_{DME})/K_{P,4}]}{(1+2\sqrt{K_{MeOH}^{ad}C_{MeOH}}+K_{H_2O,\,DME}^{ad}C_{H_2O})^4} \quad (8)$$

The units of the reaction rate (r), fugacity, and concentration are mol/(g_{cat}·s), Pa, and mol/cm^3, respectively. The symbols k, K_i^{ad}, and $K_{P,j}$ represent the reaction rate constant, adsorption equilibrium constant of species i, and reaction equilibrium of reaction j, respectively. The kinetic parameters used in this work are listed in Table 1.

2. Process Configuration

A mixture of coke oven gas and FINEX tail gas from a steelmaking plant at 25 °C and 1 atm was considered as the feed (molar fraction of $H_2/CO/CO_2/CH_4/N_2$=51/8/8/22/11). The flow rate was set as 115,000 kg/h, corresponding to a DME production of approximately 300 TPD. For the DME synthesis reaction, the feed was compressed at the reactor inlet temperature of 250 °C and pressure of 5 MPa. The tubes have a diameter of 1 inch and a length of 10 m. The number of tubes was determined so that the space veloc-

Table 1. Kinetic parameters estimated in our previous work [4]

Kinetic parameters	Pre-exponential factors	Units	Activation energy/ Heat of adsorption	Units
k_{CO}	2.95×10^{-3}	mol/(g_{cat}·s·$Pa^{1.5}$)	115,305	J/mol
k_{WGS}	2.19×10^{2}	mol/(g_{cat}·s·Pa)	119,331	J/mol
k_{DME}	1.41×10^{10}	mol/(g_{cat}·s)	123,186	J/mol
$K_{CO_2}^{ad}$	1.05×10^{-12}	1/Pa	−71,921	J/mol
$K_{H_2}^{ad}$	1.39×10^{-3}	1/Pa	−5,035	J/mol

ity was approximately 3,000 L/(kg_{cat}·h) for all the case studies, resulting in similar DME production rates. To prevent the peak temperature from exceeding the threshold value (290 °C in the present study, above which the catalytic deactivation becomes significant), the utility temperature in the reactor jacket was set as 200 °C. The details of the number of tubes for each case are provided in the Results and Discussion section.

The developed kinetic model was implemented in a process simulator (UniSim Design Suite, Honeywell Inc.), in which the non-random two-liquid (NRTL) model and Soave-Redlich-Kwong model were used as the liquid activity and gas-phase thermodynamic models, respectively.

2-1. Base Case

The base case represents the open-loop process proposed in our previous work [4], consisting of a single-step DME synthesis reactor and two distillation columns (Fig. 1). The reactor effluent was separated into light gas (CO, H_2, CH_4, N_2) at the top and a mixture of DME, MeOH, and H_2O at the bottom of the first column. The column pressure was 5 MPa. The specifications for the condenser and reboiler were less than 0.1 wt% of DME and less than 0.1 wt% of CO_2, respectively. The DME was separated at the top of the second column with a purity higher than 99.5 wt%. The column pressure was 1 MPa. The condenser and reboiler were set to have less than 0.1 wt% of MeOH and less than 0.1 wt% of DME, respectively. The temperatures of the condensers and reboilers are listed in Table 2.

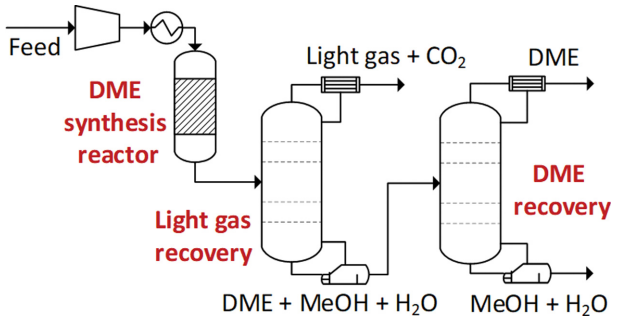

Fig. 1. Basic flow diagram of the base case.

2-2. Case 1: Application of Two Flash Drums for the Recovery of Light Gas

The condenser temperature of the "Light gas recovery" unit in the base case was very low (−65.86 °C), indicating that a cryogenic operation is required to condense both the light gas and CO_2. To reduce the amount of distillate under cryogenic conditions, Case 1 was proposed to have a DME synthesis reactor, two flash vessels, and two distillation columns, based on the reported processing scheme [7]. Depending on the existence of the recycled stream, three subclasses were considered in Case 1: open loop (Case 1-O), recycling of both light gas and CO_2 (Case 1-R1, Fig. 2(a)), and recycling of hydrogen only (Case 1-R2, Fig. 2(b)).

The flash separation of the reactor effluent was conducted at

Table 2. Temperature, pressure, and flow rate for each unit

			Light gas recovery	DME recovery
Base case			5 MPa Top: −65.86 °C Bottom: 193.6 °C	1 MPa Top: 45.24 °C Bottom: 159.8 °C
Case 1		1st/2nd flash	CO_2 recovery	DME recovery
	1-O	5 MPa 32 °C/−65 °C	5 MPa Top: −26.34 °C Bottom: 194.9 °C	1 MPa Top: 45.43 °C Bottom: 160 °C
	1-R1	5 MPa 32 °C/−65 °C	5 MPa Top: −30.34 °C Bottom: 205.9 °C	1 MPa Top: 45.42 °C Bottom: 163.2 °C
	1-R2	5 MPa 32 °C/−65 °C	5 MPa Top: −28.56 °C Bottom: 206.6 °C	1 MPa Top: 45.41 °C Bottom: 162.5 °C
Case 2		Absorber	DME recovery	DME purification
	2-O	5 MPa, 25 °C Solvent: 4,371 kmol/h	1 MPa Top: 42.02 °C Bottom: 161.4 °C	1 MPa Top: 10.00 °C Bottom: 43.28 °C
	2-R1	5 MPa, 25 °C Solvent: 33,006 kmol/h	Top: 39.79 °C Bottom: 166.1 °C	1 MPa Top: 10.00 °C Bottom: 42.81 °C
	2-R2	5 MPa, 25 °C Solvent: 7,545 kmol/h	1 MPa Top: 42.71 °C Bottom: 163.4 °C	1 MPa Top: 10.00 °C Bottom: 42.49 °C

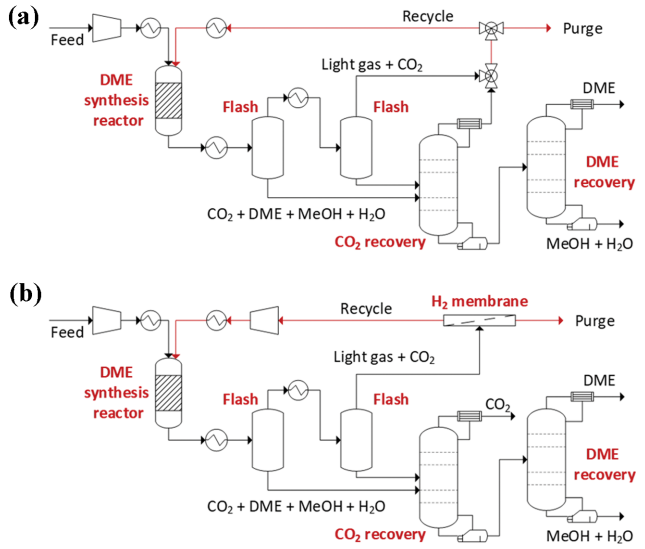

Fig. 2. Basic flow diagrams of (a) Case 1-R1 for the recycling of both light gas and CO_2; and (b) Case 1-R2 for the recycling of hydrogen after passing through the membrane. Case 1-O represents the open-loop case without red lines in the diagrams.

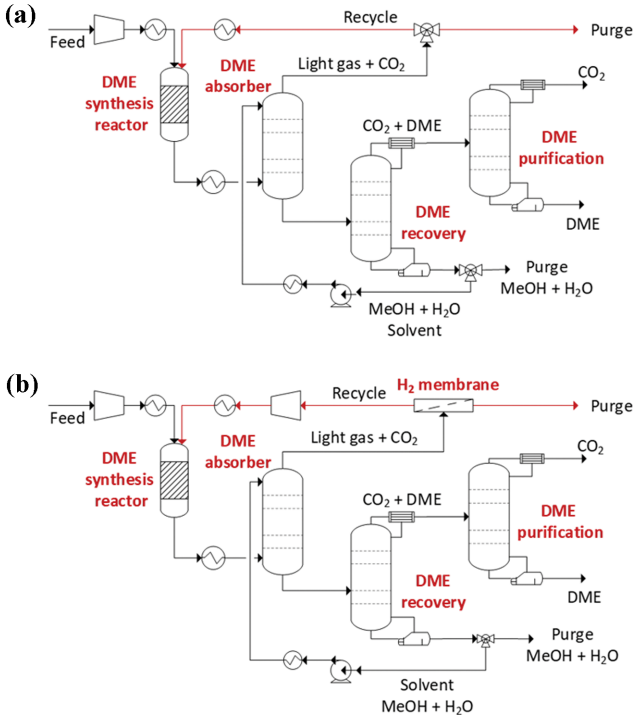

Fig. 3. Basic flow diagram of (a) Case 2-R1 for the recycling of both light gas and CO_2, and (b) Case 2-R2 for the recycling of hydrogen after passing through the membrane. Case 2-O represents the open-loop case without red lines in the diagrams.

32 °C and 5 MPa in the first flash vessel. The vapor stream was fed to the second flash drum at −65 °C so that it had less than 1 wt% DME. The final vapor stream consisted of light gas (CO, H_2, CH_4, and N_2) and CO_2 (less than half of the amount in the reactor effluent). The light gas and part of CO_2 were subjected to cryogenic cooling at −65 °C, whereas the base case required both the light gas and CO_2 to be cooled at −65.86 °C.

The remaining CO_2 at the bottom of the two flash drums was recovered in the first column ("CO_2 recovery" unit). The column pressure was 5 MPa. The specifications for the condenser and reboiler were less than 0.1 wt% of DME and less than 0.1 wt% of CO_2, respectively. Pure DME was separated at the top of the second column ("DME recovery" unit). The column pressure was 1 MPa. The specifications for the condenser and reboiler were less than 0.1 wt% of MeOH and less than 0.1 wt% of DME, respectively. However, although the condenser temperature of the CO_2 recovery column remained low (approximately −30 °C), it was still higher than the temperature in the base case (−65.86 °C), resulting in the decreased utility costs for the cryogenic operation. A detailed quantitative comparison will be conducted in the next section.

In Case 1-R1, light gas and CO_2 (sum of the vapor stream of the flash vessels and the top stream of the CO_2 recovery column) were recycled at a recycled-to-purge stream ratio of 9. A heater was used to increase the temperature of the recycled stream. In Case 1-R2, a membrane was used to selectively separate hydrogen from the vapor stream of the flash drum. The membrane was simulated using the reported data for the polysulfone membrane [13], in which the conditions for the highest hydrogen purity were considered in the modeling. The feed conditions for the membrane were 25 °C and 0.91 MPa. A compressor and cooler were used to compress the pressure of the recycled hydrogen stream because the pressure of the permeate in the membrane was set as 0.11 MPa.

2-3. Case 2: Application of a MeOH-based Absorber

Because Case 1 is still based on the cryogenic operation for the separation of light gas and CO_2, the flash drums were replaced by a MeOH-based absorber in Case 2 [14] (see the basic flow diagram in Fig. 3). Case 2 also has three subclasses: open loop (Case 2-O), recycling of both light gas and CO_2 (Case 2-R1, Fig. 3(a)), and recycling of hydrogen only (Case 2-R2, Fig. 3(b)). The recycled-to-purge stream ratio was 9 in Case 2-R1. The temperature and pressure for the membrane in Case 2-R2 were the same as in Case 1-R2.

Both the reactor effluent and absorbent at the inlet of the absorber have different concentrations of MeOH. As shown in Fig. S1 in the Supporting Information, when the MeOH concentration of the absorbent at the inlet is too low, the concentration at the outlet increased because of the larger amount of MeOH in the reactor effluent, thus requiring H_2O in the makeup stream. On the other hand, an extremely high MeOH concentration in the absorbent at the inlet required a makeup stream containing MeOH. Therefore, the MeOH concentration of the absorbent at the inlet was determined to be 18.2% in the open-loop case (Case 2-O) because no makeup stream was required. Based on the thermodynamic model in the simulator (NRTL for the liquid phase and SRK for the vapor phase), when the 18.2% MeOH solution was used, light gas and most of the CO_2 (more than 98% of total CO_2) were separated at the top of the absorber, while DME and approximately 2% of the total CO_2 were absorbed in the solution. The operating temperature and pressure were 25 °C and 5 MPa, respectively, while the flow rate of the MeOH absorbent solution was 89,940 kg/h (4,371 kmol/h). Because three subclasses in Case 2 have different syngas

conversion and MeOH selectivity owing to the different reactor inlet concentrations by recycling, the MeOH concentration of the absorbent at the inlet was determined as 11.8% and 15.3% for Cases 2-R1 and 2-R2, respectively, and the corresponding flow rates were 649,800 kg/h (33,010 kmol/h) and 152,700 kg/h (7,570 kmol/h).

In the first column ("DME recovery" unit), MeOH and H_2O were recovered at the bottom at 1 MPa and recycled to the absorber after the pressure was increased to 5 MPa (operating pressure of the absorber) by a pump. Thus, the purpose of the DME recovery unit is two-fold: the separation of DME and recovery of the absorbent. Because of the latter, the capacity of the reboiler in Case 2 was higher than that of Case 1, where the MeOH and H_2O produced in the reactor were separated (approximately one-tenth in the open-loop case).

Although DME was recovered in the first column, the stream contained a small amount of CO_2; hence, the DME purity was below the threshold value (99.5 wt%) and was sent to the second column for further purification ("DME purification" unit). The column pressure and condenser temperature were set as 1 MPa and 10 °C, respec-

Table 3. Correlations for the purchase cost

Equipment	Purchase cost [$]	Reference
Heat exchangers, Coolers, Reboilers, Reactor	$C_p=(CEPCI/500)F_MF_LF_PC_B$ $C_B=\exp[11.0545-0.9228\ln(A)+0.09861(\ln A^2)$ (for Fixed-head) $C_B=\exp[11.967-0.8709\ln(A)+0.09005(\ln A)^2)$ (for Kettle vaporizer) $150<A\ (ft^2)<12{,}000$	[16]
Pumps	$C_p=(CEPCI/500)F_TF_M\exp[9.7171-0.6019\ln(S)+0.0519(\ln S^2)]$ $S=(\text{flowrate [gallon]})(\text{pump head[ft]})^{0.5}$ $400<S<100{,}000$	
Pressure vessels, Distillation columns	$C_p=(M\&S/280)(101.9D^{1.066}H^{0.82}F_MF_p)$	[15]
Distillation column trays	$C_p=(M\&S/280)(4.7D^{1.55}H(F_s+F_t+F_M))$	
Gas compressors	$C_p=(CEPCI/342.5)6.49(HP)^{0.62}$ [K$] 200<HP<30,000, centrifugal compressor	[17]

C_p: purchased equipment cost [$]; CEPCI: Chemical Engineering Plant Cost Index; M&S: Marshall & Shift index; F_d: design parameter; F_p: pressure parameter; F_M: material parameter; A: area; bhp: brake horsepower; D: diameter [ft]; H: tray stack height [ft]; F_S: tray spacing parameter; F_t: tray-type parameter; S: size factor

Table 4. Ratio factors for total capital investment calculation [18]

Item		Ratio factor (RF_i)
Direct cost	Purchase cost	1
	Installation cost	0.47
	Instrumentation and controls	0.36
	Piping	0.68
	Electrical systems	0.11
	Buildings	0.18
	Yard improvements	0.1
	Service facilities	0.7
Total direct costs (TDC)		Σ Direct cost
Indirect cost	Engineering and supervision	0.33
	Construction expenses	0.41
	Legal expenses	0.04
	Contractor fee	0.22
	Contingency	0.44
Total indirect costs (TIC)		Σ Indirect cost
Fixed capital investment (FCI)		TDC+TIC
Working capital (WC)		0.89
Total capital investment (TCI)		FCI+WC

Table 5. Utility and methods for TPC calculation

	Item	Assumptions & correlations	Reference
Feed	Byproduct gas	3 $/MMBTU (Equal to natural gas price)	[19]
Utilities	Purge light gas	3 $/MMBTU (Equal to natural gas price)	
	Steam	9.83 $/GJ	
	Cooling water	0.013583 $/ton	
	Electricity	0.0693 $/kWh	
	Reactor utility	$7.0e^{-7}*Q_H^{-0.9}*T^{0.5}*(CEPCI)+6.0e^{-8}*T^{0.5}*$(fuel cost [$/GJ])	[20]
	Refrigerant	Exp[2.452−0.01863T(°C)], $/GJ (T<−25 °C)	[21]
		$0.6*Q_C^{-0.9}*T^{-3}*(CEPCI)+1.1e^{6}*T^{-3}*$(fuel cost [$/GJ]) (−25 °C<T<0 °C)	[20]
	Boiling feed water	2.450 $/ton	[22]
Operation & maintenance	Operating labor (OL)	60,000 $/labor/year, 10 labor/shift, 3 shift/day	[15]
	Supervisory & clerical labor (S&C)	OL×0.2	
	Maintenance & repairs (M&R)	FCI×0.06	
	Operating supplies	M&R×0.15	
	Laboratory charges	OL×0.15	
Others	Depreciation	(TCI−0.05×TCI)/20 (5 % salvage value, 20 year)	
	Patents & royalties	TPC×0.01	
	Local taxes & insurance	FCI×0.02	
	Plant overhead costs	(OL+S&C+M&R)×0.6	
	Administration	(OL+S&C+M&R)×0.2	
	Distribution & selling	TPC×0.05	
	Research & development	TPC×0.04	
Total production cost (TPC)	Raw materials+Utilities+Operation & maintenance+Others		

tively. A DME purity of 99.5 wt% was achieved at the bottom.

As shown in Table 2, the operating temperatures of the absorber and DME recovery unit were 25 °C and approximately 40 °C, respectively. Although DME purification required a refrigerant at 10 °C, the very small amount of distillate means that the cost of the cryogenic operation in Case 2 was much lower than those of the base case and Case 1.

3. Estimation of Total Capital Investment and Total Production Cost

The techno-economics of the entire process, including the total capital investment (TCI) and total production cost (TPC), was evaluated, i.e., the feed gas compression, DME synthesis, recycle compressor or heater, membrane, and other utilities such as feed gas, purge light gas, cooling water, electricity, and steam generators. First, the equipment cost was estimated using the cost correlation functions reported in the literature [15-17]. The cost correlation functions of the purchased equipment cost are listed in Table 3.

The TCI was determined using Eq. (9), where I_E and RF_i denote the purchased equipment cost and ratio factors, respectively [18].

Table 6. Economic assumptions for the estimation of the minimum selling price

Items	Values
Base year	2,021
Operating hours [h]	7,920
Recovery period [y]	20
Discount rate [%]	8

$$TCI = I_E \times \left(1 + \sum_{i=1}^{n} RF_i\right) \quad (9)$$

The values of the ratio factors used to calculate the TCI are listed in Table 4. The assumptions and correlations used to calculate the TPC are listed in Table 5. The unit prices of feed gas and light gas were assumed to be equal to the price of natural gas (NG) because both streams can be used as fuel for steelmaking plants despite their different compositions from NG.

Finally, the minimum selling price (MSP) was estimated as the DME selling price that yields a net present value equal to zero. The

Table 7. Local and overall values for each case

		Base	1-O	1-R1	1-R2	2-O	2-R1	2-R2
Local	Tube number	9,600	9,600	55,000	18,000	9,600	55,000	17,000
	SV [L/(kg_{cat}·h)]	3,000	3,000	3,011	2,964	3,000	3,003	3,130
	$H_2/(2CO+3CO_2)$	1.275	1.275	2.263	2.500	1.275	2.299	2.102
	CO conversion [%]	87.50	87.50	76.75	94.57	87.50	79.81	92.25
	CO_2 conversion [%]	6.052	6.052	28.42	47.88	6.052	29.13	41.47
	DME selectivity [%]	77.23	77.23	69.42	71.51	77.23	72.52	71.22
	DME yield [%]	26.08	26.08	21.02	34.30	26.08	23.25	29.90
	DME production [kg/h]	12,894	12,894	31,231	21,543	12,894	25,574	21,846
Overall	CO conversion [%]	87.50	87.50	97.05	95.15	87.50	97.35	93.05
	CO_2 conversion [%]	6.052	6.052	79.76	68.38	6.052	77.49	73.31
	DME recovery [%]	97.49	93.62	95.87	92.34	93.35	90.82	94.39
	DME purity [%]	99.69	99.73	99.68	99.69	99.50	99.50	99.50
	Carbon mass efficiency [%][a]	25.42	24.42	44.49	40.26	24.37	45.48	41.70

[a]Carbon mass efficiency was calculated as the ratio of the mass flow rate of the DME product to the mass flow rate of the CO and CO_2 in the process feed, corresponding to the overall DME yield.

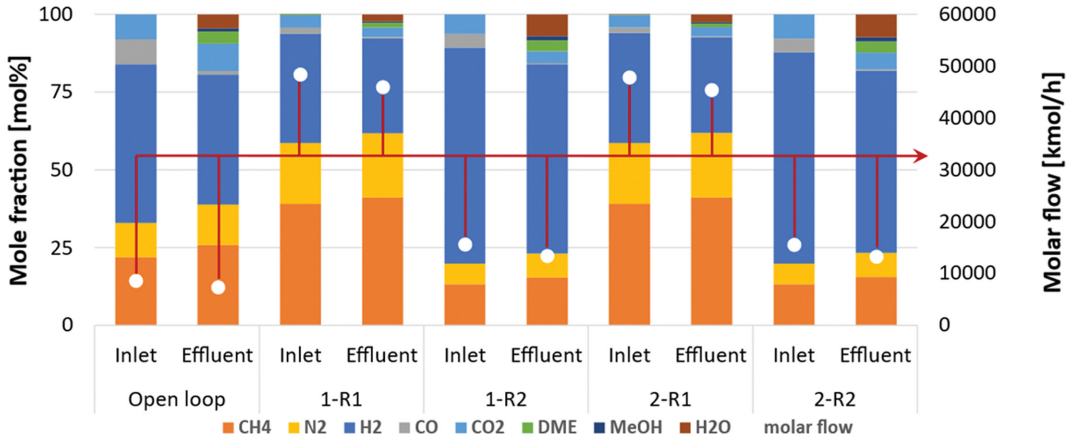

Fig. 4. Mole fraction (left axis) and molar flow rate (right axis) of the reactor inlet and outlet for each condition. "Open loop" represents the base case, Case 1-O, and Case 2-O.

economic assumptions for calculating MSP are listed in Table 6.

RESULTS AND DISCUSSION

1. Effects of the Recycled Stream

Table 7 and Fig. 4 show the simulation results for all the cases considered in the present study. Detailed heat and mass balances are provided in the Supporting Information. The local values represent the calculations based on the inlet and outlet of the reactor. The overall values were calculated using the feed stream (process input) and all the output streams in the process (process outputs). As explained in the previous section, the number of tubes required to maintain the space velocities at approximately 3,000 L/(kg_{cat}·h) was determined. The actual numbers are listed in Table 7. As the recycled stream of light gas and CO_2 was introduced into the process (R1 cases; Cases 1-R1 and 2-R1), the molar flow rate at the reactor inlet significantly increased (white symbols in Fig. 4), while the number of tubes increased proportionally with the flow rate (approximately six times; 9,600 in the open loop vs. 55,000 in the R1 cases). When only hydrogen was recycled (R2 cases; Cases 1-R2 and 2-R2), the inlet flow rate increased approximately two-fold along with the number of tubes.

Despite similar space velocity between the cases, local CO conversions for R1 cases slightly decreased, while local CO_2 conversions increased owing to the increased CO_2 hydrogenation rate caused by the increased amount of hydrogen (cf. $H_2/(2CO+3CO_2)$ in Table 7). When the recycled stream consisted of pure hydrogen (R2 cases), in addition to the increased amount of hydrogen, the decrease in inert gas at the reactor inlet (cf. molar fractions of CH_4 and N_2 in Fig. 4) increased the partial pressures of the reactants; thus, both local CO and CO_2 conversions were higher than those in the R1 cases. However, with regard to DME production, which is proportional to the conversion as well as the flow rates of the reactants at the reactor inlet, the R1 cases produced more DME than the R2 cases because of the increased amount of reactants in the recycled stream.

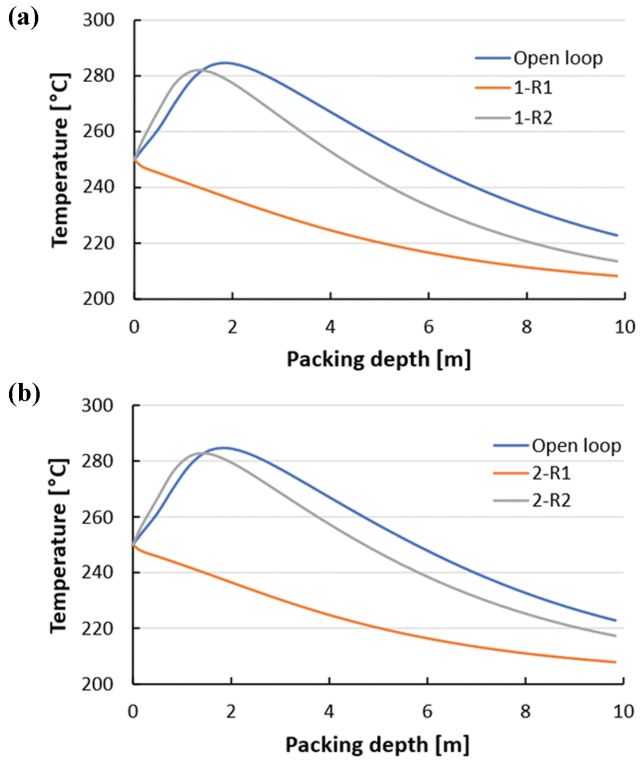

Fig. 5. The temperature profiles of (a) Case 1 and (b) Case 2.

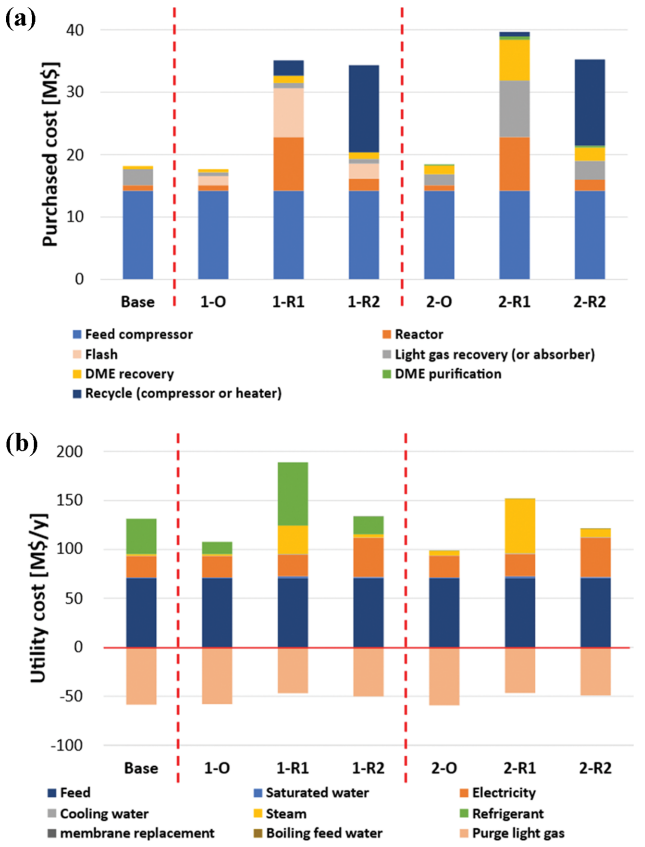

Fig. 6. (a) Purchased equipment cost [M$] and (b) utility cost [M$/y] for each case.

The overall CO conversion for both R1 and R2 cases increased by approximately 10% (the lowest is 6.3% for Case 2-R2, and the highest is 11.3% for Case 2-R1), while a significant increase in the overall CO_2 conversion was observed for the recycled cases. This feature indicates that the introduction of the recycled stream significantly influences the utilization of CO_2 rather than CO. Thus, the increased CO_2 utilization led to a significant decrease in the amount of CO_2 released to the environment.

Fig. 5 shows the temperature profiles of the reactor in each case. The open loop and R2 cases have similar profiles because the compositions at the reactor inlet (cf. molar fractions of the inlet for the open loop, 1-R2, and 2-R2 cases in Fig. 4) were similar for the same space velocity. However, the recycling of both the unreacted reactants and inert gases (R1 cases) increased the proportion of inert gas at the reactor inlet, resulting in increased heat absorption by the inert gases and the removal of peak temperatures in Cases 1-R1 and 2-R1.

2. Techno-economic Evaluation

As shown in the previous section, the utility cost of cryogenic separation for light gas and CO_2 may decrease in Case 1, and a further decrease in Case 2 with the application of the absorber at atmospheric temperature. However, a large amount of absorbent must be recovered in the DME recovery column at a potentially high operating cost of the reboiler. This result indicates a tradeoff between Cases 1 and 2. The application of the recycled stream increases CO_2 conversion and carbon efficiency at the expense of the purchase cost of the reactor (the increase in the number of tubes was considered for the same space velocity). The different recycling strategies (R1 vs. R2 cases) may also require a tradeoff: R1 exhibited superior thermal behavior in the reactor (no peak temperature) because of the high fraction of inert gases; however, a large number of catalytic tubes was required. Therefore, considering the many tradeoffs between the cases, the techno-economics of the cases were calculated for quantitative comparison.

As shown in Fig. 6(a), the purchase cost of the feed compressor, which was required to increase the feed pressure from atmospheric to 5 MPa, contributed the most to the total purchase cost for all cases, accounting for approximately 80% in the open-loop cases. By applying the recycled stream, the total purchase cost increased by approximately twice that of the open-loop case. In Case 1-R1, the recycled stream, including the unreacted reactants and a large amount of inert gases, increased the costs of the reactor (orange bar) and the two flash drums (pink bar). In Case 1-R2, a large compressor capacity was required to increase the pressure of the recycled hydrogen from 0.11 to 5 MPa. In Case 2-R1, the recovery of the absorbent in the DME recovery column increased the size of the reboiler and the corresponding purchase cost (yellow bar). Because the amount of recycled stream in Case 2-R2 was lower than that in Case 2-R1, the cost of the DME recovery column was lower than that in Case 2-R1. Overall, the application of the recycled stream increased the production rate and CO_2 reduction, but also increased the total purchase cost. Although Case 2-R1 had the highest cost, the difference between the recycled cases was not significant.

The feed price accounted for the largest proportion of the util-

ity cost (Fig. 6(b)). However, because the purge gas is expected to be used as the fuel for furnaces in the steelmaking process, its cost (pink bar with negative values) might cancel out the high feed cost. In the base case, a refrigerant was used to condense both light gas and CO_2, resulting in high utility costs (green bar), while the application of additional flash drums for the separate recovery of light gas and CO_2 in Case 1-O reduced utility costs by approximately one-third. However, the recycled stream increased the amount of condensation; hence, Cases 1-R1 and 1-R2 showed increased utility costs. In Case 1-R1, heating of the recycled stream (from subzero to 250 °C) increased the cost of steam (yellow bar). Although the smaller amount of recycled stream in Case 1-R2 compared with that in Case 1-R1 reduced refrigerant and steam costs, the compression of the recycled hydrogen increased the cost of electricity (orange bar).

Both the open and recycled cases in Case 2 (Cases 2-O, 2-R1, and 2-R2) offset the cost of the refrigerant owing to the application of the absorber at 25 °C. The increased capacity of the reboiler for the recovery of the absorbent increased the cost of steam compared with the base case. Case 2-R1 showed a significant increase in the cost of steam owing to the increased amount of recycled stream. Case 2-R2 showed a high electricity cost resulting from the compression of the recycled hydrogen, as in Case 1-R2.

A comparison of Cases 1 and 2 showed that Case 2 has lower utility costs than Case 1 because the unit price of the steam was lower than that of the refrigerant. Therefore, Case 2-R2 exhibited the lowest utility cost among the recycled cases.

With the MSP based on the purchase and utility costs shown in Fig. 6, Case 1-R1 resulted in the highest value. The price decreased in the following order: base case, Case 2-R1, Case 1-R2, and Case 2-R2 (the lowest MSP) (see the values along the red dotted lines in Fig. 7).

As discussed in Fig. 6, the costs of steam, electricity, and feed had the largest contributions to the total cost; hence, their effects on the MSP were evaluated. As shown in Fig. 7(a), R1 cases (Cases 1-R1 and 2-R1) showed higher sensitivity to the steam price than R2 cases (Cases 1-R2 and 2-R2) because the former required the heating of recycled stream. Case 2-R1 was more sensitive to the steam price than Case 1-R1 because steam was also used in the recovery of the absorbent. However, despite the differences in sensitivity to the steam price, Case 2-R2 showed the lowest MSP among all the steam prices.

The compression of the feed resulted in the sensitivity of the MSP on the electricity price for all cases, as shown in Fig. 7(b). The sensitivity of R2 cases (dotted blue and green lines) was higher than that of R1 cases (solid blue and green lines) because additional compression of the recycled hydrogen was required. Although the MSP of Case 1-R2 exceeded that of Case 2-R1 at very high electricity prices, the lowest MSP was observed for Case 2-R2, regardless of electricity prices.

The amount of feed remained constant for all the cases, while the varying amounts of purge stream resulted in differences in the utility cost (pink bar in Fig. 6(b)). However, the effects of the different amounts of purge stream did not significantly influence the sensitivity to the feed price, as shown by the similar slopes between the cases in Fig. 7(c).

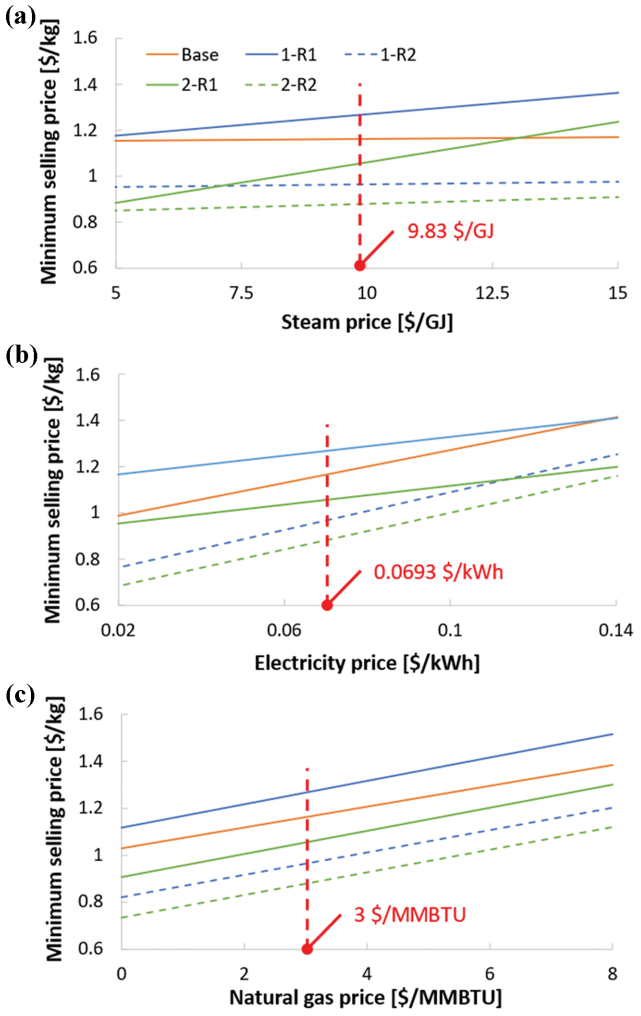

Fig. 7. Effects of (a) steam price [$/GJ], (b) electricity price [$/kWh], and (c) natural gas price [$/MMBTU] on the minimum selling price of each case. Red dots represent the value considered in the present study.

Noteworthy is that the minimum selling price is influenced by the discount ratio; the NPV profile for Case 2-R2 is provided in Fig. S9 in the Supporting Information.

CONCLUSIONS

Although the physical mixing of two catalysts for MeOH synthesis and dehydration results in high CO and CO_2 conversion to DME, the reactor effluents also contain many different species (e.g., unreacted reactants, inert gas, and product) that must be separated to obtain high-purity DME. Two different separation trains (flash drums for the separation of light gases followed by two columns for the separation of CO_2 and DME; and the application of an absorber for the separation of light gas and CO_2 under mild temperatures), and two different recycling strategies (recycling with and without further separation of hydrogen by a membrane) were considered. Based on the detailed kinetic reaction rates, each case showed different compositions of the reactor effluent, and the operating conditions of the separation trains were determined. The

results showed that both separation trains with the recycled stream led to increased conversion, especially the overall CO_2 conversion for increased CO_2 reduction, and an increase in the DME production rate, along with higher purchase and utility costs. The tradeoffs between cases were discussed, and techno-economic analyses quantitatively showed that the use of an absorber and the recycling of only hydrogen results in the lowest MSP. Further study on the sensitivity of the MSP to the unit price was conducted. Despite varying sensitivities, the case for the lowest MSP was maintained. It is concluded that the process models proposed in the present study can accurately predict the kinetic behavior as well as the effect of the separation train and process configuration on the feasibility of the process.

ACKNOWLEDGEMENTS

This research was supported by the National Research Foundation of Korea (NRF), funded by the Ministry of Science and ICT of the Republic of Korea (No. 2021M3I3A1084300). G. Kim acknowledges that this work was supported by the Korea Institute of Energy Technology Evaluation and Planning (KETEP) and the Ministry of Trade, Industry & Energy (MOTIE) of the Republic of Korea (No. 20212010100040).

SUPPORTING INFORMATION

Additional information as noted in the text. This information is available via the Internet at http://www.springer.com/chemistry/journal/11814.

REFERENCES

1. A. Masudi, N. W. Che Jusoh and O. Muraza, *J. Cleaner Prod.*, **277**, 124024 (2020).
2. S. H. Park and C. S. Lee, *Energy Convers. Manage.*, **86**, 848 (2014).
3. W.-H. Chen, C.-L. Hsu and X.-D. Wang, *Energy*, **109**, 326 (2016).
4. H. Park, Y. Woo, H. S. Jung, G. Kim, J. W. Bae and M.-J. Park, *J. Cleaner Prod.*, **326**, 129367 (2021).
5. Z. Azizi, M. Rezaeimanesh, T. Tohidian and M. R. Rahimpour, *Chem. Eng. Process.*, **82**, 150 (2014).
6. G. Leonzio, *J. CO_2 Util.*, **27**, 326 (2018).
7. J. Chung, W. Cho, Y. Baek and C.-H. Lee, *Trans. Korean Hydrogen New Energy Soc.*, **23**, 559 (2012).
8. Y. Zhang, S. Zhang and T. Benson, *Fuel Process. Technol.*, **131**, 7 (2015).
9. L. R. Clausen, B. Elmegaard and N. Houbak, *Energy*, **35**, 4831 (2010).
10. C. Mevawala, Y. Jiang and D. Bhattacharyya, *Appl. Energ.*, **238**, 119 (2019).
11. N. Park, M.-J. Park, Y.-J. Lee, K.-S. Ha and K.-W. Jun, *Fuel Process. Technol.*, **125**, 139 (2014).
12. K. L. Ng, D. Chadwick and B. A. Toseland, *Chem. Eng. Sci.*, **54**, 3587 (1999).
13. G. J. Kwak, G. U. Kim, Y. J. Lee and S. C. Kang, KOR. Patent, KR102316885B1 (2021).
14. C. Mevawala, Y. Jiang and D. Bhattacharyya, *Appl. Energ.*, **204**, 163 (2017).
15. J. M. Douglas, *Conceptual design of chemical processes*, McGraw-Hill, New York (1988).
16. W. D. Seider, J. D. Seader and D. R. Lewin, *Product & process design principles: synthesis, analysis and evaluation*, 3rd edn. John Wiley & Sons, New Jersey (2009).
17. S. M. Walas, *Chemical process equipment: selection and design*, Butterworths, Boston (1988).
18. M. S. Peters, K. D. Timmerhaus and R. E. West, *Plant design and economics for chemical engineers*, McGraw-Hill, New York (2003).
19. S. Kim, Y. Kim, S.-Y. Oh, M.-J. Park and W. B. Lee, *J. Nat. Gas Sci. Eng.*, **96**, 104308 (2021).
20. G. D. Ulrich and P. T. Vasudevan, *Chem. Eng.*, **113**, 66 (2006).
21. W. L. Luyben, *Comput. Chem. Eng.*, **103**, 144 (2017).
22. R. Turton, R. C. Bailie, W. B. Whiting and J. A. Shaeiwitz, *Analysis, synthesis and design of chemical processes*, Prentice Hall, New Jersey (2008).

Supporting Information

Techno-economic analysis of the integrated DME production process: Effects of different separation trains and recycling strategies

Hyeon Park*, Jong Wook Bae, Gookhee Kim***,†, and Myung-June Park*,****,†**

*Department of Energy Systems Research, Ajou University, Suwon 16499, Korea
**School of Chemical Engineering, Sungkyunkwan University (SKKU), Suwon 16419, Korea
***Research Institute of Industrial Science & Technology (RIST), Pohang 37673, Korea
****Department of Chemical Engineering, Ajou University, Suwon 16499, Korea
(*Received 19 April 2022 • Revised 29 June 2022 • Accepted 19 July 2022*)

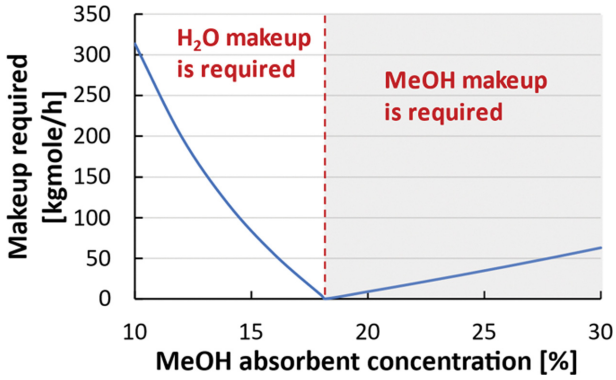

Fig. S1. Amount of the makeup required as a function of the MeOH absorbent concentration at the inlet of the absorber. The region of the white background represents H_2O needs to be made up while the gray area indicates MeOH needs for makeup.

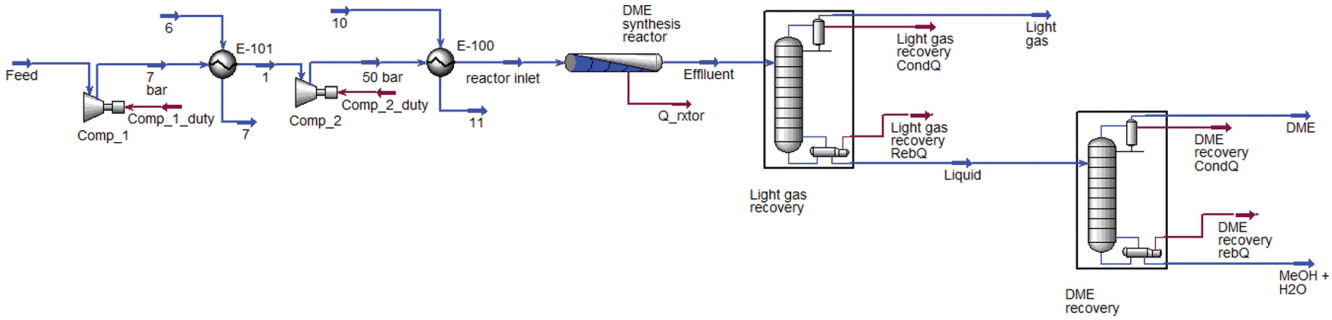

Fig. S2. Process scheme of the base case.

Table S1. Heat and mass balance of the base case

Name	Feed	Reactor inlet	Effluent	Light gas	Liquid	DME	MeOH+H_2O
Temperature [°C]	25.0	250	222.6	−65.86	193.6	45.24	159.8
Pressure [kPa]	101.3	5,000	5,000	5,000	5,000	1,000	1,000
Molar flow [kgmol/h]	8,581.7	8,581.7	7,297.2	6,619.4	677.88	273.81	404.07
Mass flow [kg/h]	115,000	115,000	46,765.8	93,947.6	21,053.0	12,608.8	8,444.18
H_2 [kg/h]	8,823.376	8,823.376	6,150.105	6,150.105	1.89E-11	1.89E-11	8.08E-28
CH_4 [kg/h]	30,288.48	30,288.48	30,288.48	30,288.48	6.53E-06	6.53E-06	6.37E-27
CO [kg/h]	19,230.29	19,230.29	2,404.485	2,404.485	1.26E-07	1.26E-07	2.29E-25
N_2 [kg/h]	26,443.82	26,443.82	26,443.82	26,443.82	5.68E-10	5.68E-10	1.13E-26
CO_2 [kg/h]	30,214.03	30,214.03	28,385.51	28,355.75	29.75743	29.75743	1.82E-18
DME [kg/h]	0	0	12,893.85	304.9472	12,588.91	12,570.31	18.59534
MeOH [kg/h]	0	0	2,643.877	0.010664	2,643.866	8.771873	2,635.094
H_2O [kg/h]	0	0	5,790.488	8.30E-05	5,790.488	2.41E-03	5,790.486

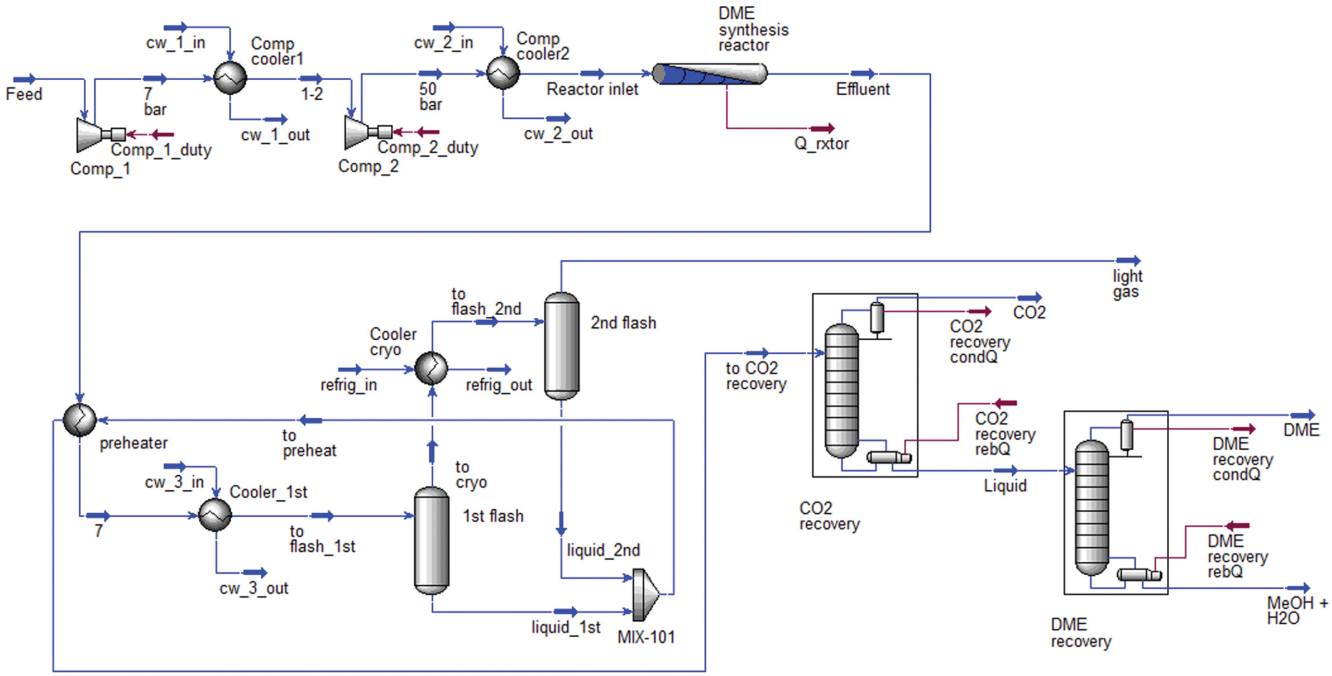

Fig. S3. Process scheme of Case 1-O.

Table S2. Heat and mass balance for Case 1-O

Name	Feed	Reactor inlet	Effluent	to flash_1st	to flash_2nd	to CO_2 recovery	Light gas	CO_2	Liquid	DME	MeOH+H_2O
Temperature [C]	25.00	250.00	222.60	32.00	−65.00	25.00	−65.00	−26.34	194.92	45.43	159.98
Pressure [kPa]	101.32	5,000.00	5,000.00	5,000.00	5,000.00	5,000.00	5,000.00	5,000.00	5,000.00	1,000.00	1,000.00
Molar flow [kgmol/h]	8,581.69	8,581.69	7,297.25	7,297.25	6,877.70	941.38	6,355.87	274.76	666.61	262.88	403.74
Mass flow [kg/h]	115,000.00	115,000.00	115,000.61	115,000.61	105,488.19	30,697.66	84,302.95	10,162.92	20,534.73	12,104.25	8,430.49
H_2 [kg/h]	8,823.38	8,823.38	6,150.12	6,150.12	6,149.35	7.03	6,143.09	7.03	0.00	0.00	0.00
CH_4 [kg/h]	30,288.48	30,288.48	30,288.48	30,288.48	30,281.91	998.47	29,290.01	998.47	0.00	0.00	0.00
CO [kg/h]	19,230.29	19,230.29	2,404.52	2,404.52	2,402.58	4.49	2,400.04	4.49	0.00	0.00	0.00
N_2 [kg/h]	26,443.82	26,443.82	26,443.82	26,443.82	26,440.51	70.43	26,373.39	70.43	0.00	0.00	0.00
CO_2 [kg/h]	30,214.03	30,214.03	28,385.54	28,385.54	28,329.42	9,092.83	19,292.71	9,072.35	20.48	20.48	0.00
DME [kg/h]	0.00	0.00	12,893.80	12,893.80	11,336.38	12,090.25	803.55	10.16	12,080.09	12,071.65	8.44
MeOH [kg/h]	0.00	0.00	2,643.86	2,643.86	410.43	2,643.70	0.16	0.00	2,643.70	12.10	2,631.60
H_2O [kg/h]	0.00	0.00	5,790.46	5,790.46	137.60	5,790.46	0.00	0.00	5,790.46	0.01	5,790.45

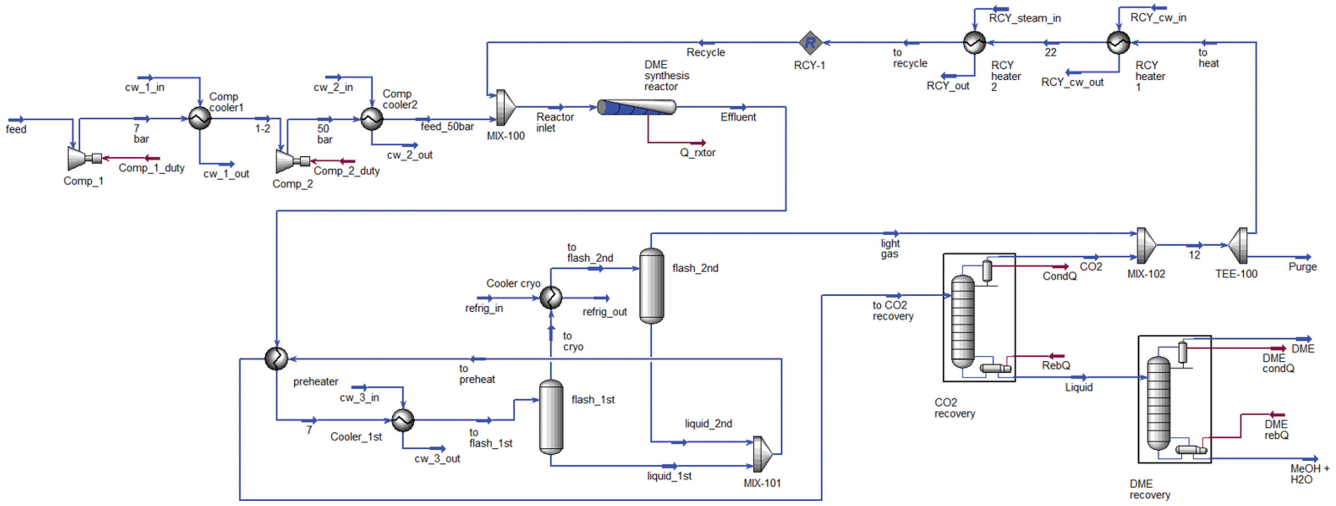

Fig. S4. Process scheme of Case 1-R1.

Table S3. Heat and mass balance for Case 1-R1

Name	Feed	Reactor inlet	Effluent	to flash_1st	to flash_2nd	to CO_2 recovery	Liquid	CO_2	DME	MeOH+ H_2O	Recycle	Purge
Temperature [C]	25.00	249.97	208.15	32.00	−65.00	25.00	206.79	−39.35	45.41	161.98	250.00	−64.90
Pressure [kPa]	101.32	5,000.00	5,000.00	5,000.00	5,000.00	5,000.00	5,000.00	5,000.00	1,000.00	1,000.00	5,000.00	5,000.00
Molar flow [kgmol/h]	8,581.69	48,323.91	45,894.91	45,894.91	44,732.40	1,917.33	1,744.39	172.94	479.27	1,265.12	39,742.23	4,415.05
Mass flow [kg/h]	115,000.00	719,248.28	719,270.51	719,270.51	695,601.09	52,981.90	47,939.81	5,042.09	22,067.62	25,872.19	604,248.28	67,133.07
H_2 [kg/h]	8,823.38	34,313.60	28,310.52	28,310.52	28,309.62	6.15	0.00	6.15	0.00	0.00	25,490.22	2,831.05
CH_4 [kg/h]	30,288.48	302,963.19	302,963.19	302,963.19	302,949.36	1,375.18	0.00	1,375.18	0.00	0.00	272,674.71	30,296.32
CO [kg/h]	19,230.29	24,329.23	5,655.45	5,655.45	5,653.80	2.77	0.00	2.77	0.00	0.00	5,098.94	565.55
N_2 [kg/h]	26,443.82	264,506.64	264,506.64	264,506.64	264,494.96	73.90	0.00	73.90	0.00	0.00	238,062.82	26,450.66
CO_2 [kg/h]	30,214.03	84,844.17	60,731.11	60,731.11	60,695.61	3,626.95	47.91	3,579.04	47.91	0.00	54,630.13	6,068.32
DME [kg/h]	0.00	8,287.55	31,230.89	31,230.89	30,060.72	22,028.56	22,023.52	5.04	21,997.62	25.90	8,287.55	920.74
MeOH [kg/h]	0.00	3.84	7,028.28	7,028.28	2,465.92	7,024.02	7,024.02	0.00	22.07	7,001.95	3.84	0.43
H_2O [kg/h]	0.00	0.05	18,844.42	18,844.42	971.10	18,844.36	18,844.36	0.00	0.02	18,844.33	0.05	0.01

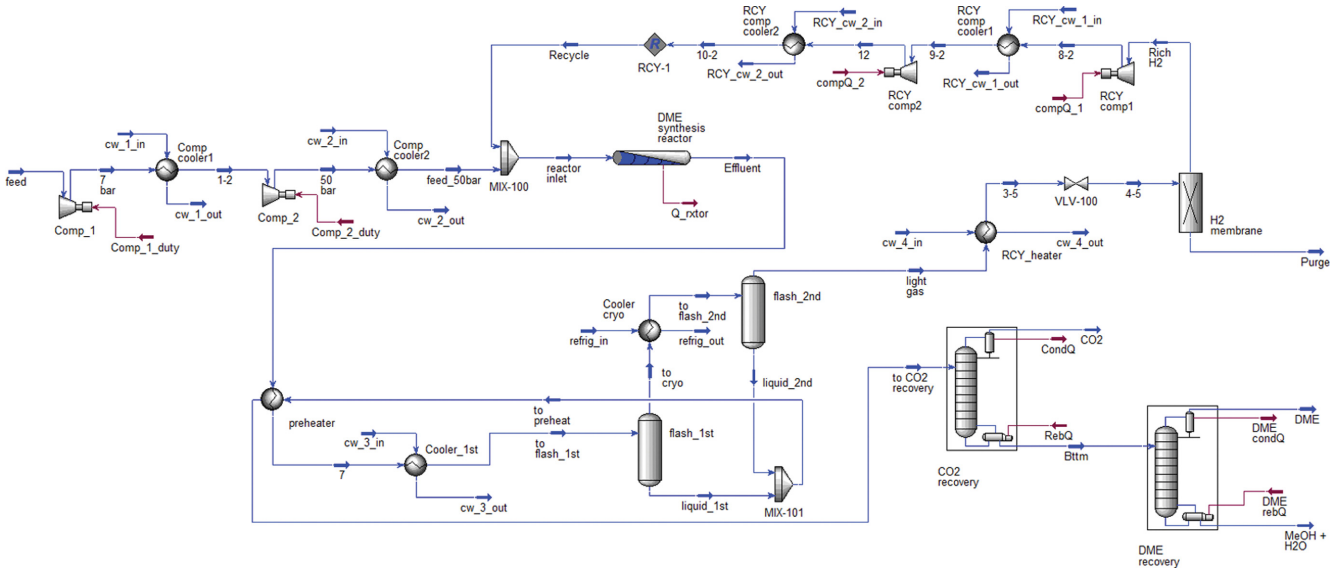

Fig. S5. Process scheme of Case 1-R2.

Table S4. Heat and mass balance for Case 1-R2

Name	Feed	Reactor inlet	Effluent	to flash_1st	to flash_2nd	to CO_2 recovery	CO_2	Bttm	DME	MeOH+ H_2O	Light gas	Purge	Recycle
Temperature [C]	25.00	249.75	213.98	32.00	−65.00	25.00	−28.45	206.57	45.41	162.49	−65.00	25.31	250
Pressure [kPa]	101.32	5,000.00	5,000.00	5,000.00	5,000.00	5,000.00	5,000.00	5,000.00	1,000.00	1,000.00	5,000.00	1,000.00	5,000
Molar flow [kgmol/h]	8,581.69	15,585.03	13,350.29	13,350.29	12,175.93	1,723.70	174.80	1,548.90	431.79	1,117.11	11,626.58	4,616.47	7,003.345
Mass flow [kg/h]	115,000.00	146,221.65	146,222.43	146,222.43	120,349.16	48,812.43	6,200.85	42,611.58	19,881.45	22,730.14	97,410.00	66,167.45	31,221.65
H_2 [kg/h]	8,823.38	21,815.58	16,371.08	16,371.08	16,368.30	11.98	11.98	0.00	0.00	0.00	16,359.10	3,353.62	12,992.2
CH_4 [kg/h]	30,288.48	33,179.49	33,179.49	33,179.49	33,169.54	695.98	695.98	0.00	0.00	0.00	32,483.51	29,592.48	2,891.01
CO [kg/h]	19,230.29	19,352.29	1,102.25	1,102.25	1,100.88	2.05	2.05	0.00	0.00	0.00	1,100.20	978.07	122.0027
N_2 [kg/h]	26,443.82	28,639.50	28,639.50	28,639.50	28,633.58	49.89	49.89	0.00	0.00	0.00	28,589.61	26,393.93	2,195.68
CO_2 [kg/h]	30,214.03	43,234.79	22,733.21	22,733.21	22,663.13	5,477.27	5,434.75	42.52	42.52	0.00	17,255.94	4,227.71	13,020.76
DME [kg/h]	0.00	0.00	21,469.36	21,469.36	17,619.24	19,847.98	6.20	19,841.78	19,819.02	22.76	1,621.37	1,621.37	0
MeOH [kg/h]	0.00	0.00	5,939.85	5,939.85	567.36	5,939.58	0.00	5,939.58	19.88	5,919.70	0.27	0.27	0
H_2O [kg/h]	0.00	0.00	16,787.70	16,787.70	227.14	16,787.70	0.00	16,787.70	0.02	16,787.68	0.00	0.00	0

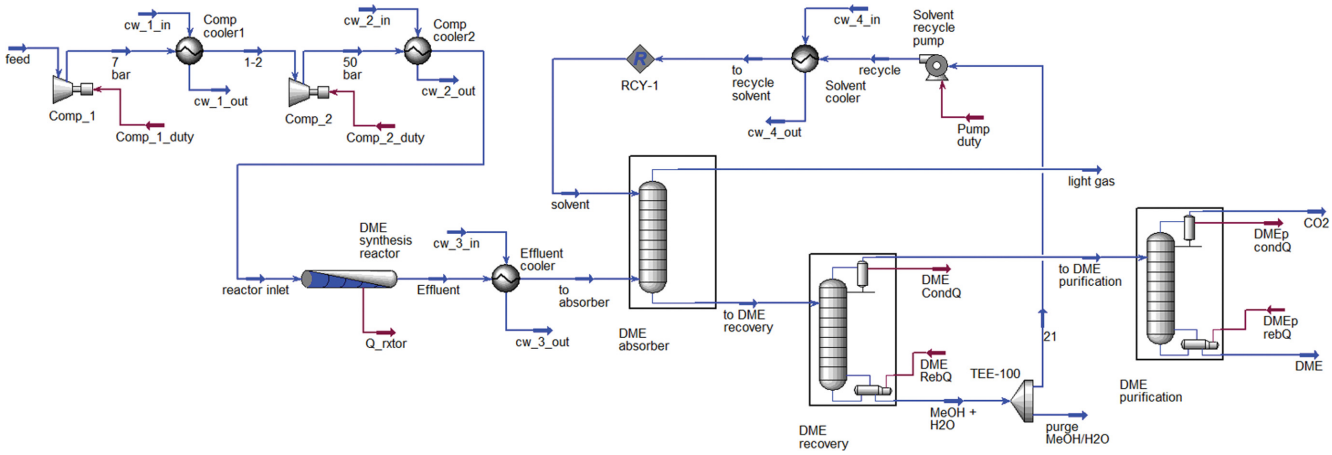

Fig. S6. Process scheme of Case 2-O.

Table S5. Heat and mass balance for Case 2-O

Name	Feed	Reactor inlet	Effluent	to DME recovery	Light gas	to DME purification	Solvent	Purge MeOH/H_2O	DME	CO_2
Temperature [C]	25.00	250.00	222.60	33.64	26.24	42.02	25.00	161.36	43.28	10.01
Pressure [kPa]	101.32	5,000.00	5,000.00	5,000.00	5,000.00	1,000.00	5,000.00	1,000.00	1,000.00	1,000.00
Molar flow [kgmol/h]	8,581.69	8,581.69	7,297.23	5,055.66	6,612.22	298.48	4,370.64	386.62	262.82	35.66
Mass flow [kg/h]	115,000.00	115,000.00	115,000.42	111,278.54	93,659.86	13,386.23	89,937.98	7,955.80	12,096.40	1,289.82
H_2 [kg/h]	8,823.38	8,823.38	6,150.10	8.05	6,142.04	8.05	0.00	0.00	0.00	8.05
CH_4 [kg/h]	30,288.48	30,288.48	30,288.48	63.41	30,225.07	63.41	0.00	0.00	1.75	61.66
CO [kg/h]	19,230.29	19,230.29	2,404.46	22.58	2,381.89	22.58	0.00	0.00	0.00	22.58
N_2 [kg/h]	26,443.82	26,443.82	26,443.82	34.54	26,409.28	34.54	0.00	0.00	0.02	34.52
CO_2 [kg/h]	30,214.03	30,214.03	28,385.48	577.36	27,808.12	577.36	0.00	0.00	45.31	532.04
DME [kg/h]	0.00	0.00	12,893.70	12,764.77	218.89	12,666.89	89.97	7.96	12,035.92	630.97
MeOH [kg/h]	0.00	0.00	2,643.87	27,725.93	378.26	13.39	25,460.32	2,252.22	13.39	0.00
H_2O [kg/h]	0.00	0.00	5,790.51	70,081.89	96.31	0.01	64,387.69	5,695.62	0.01	0.00

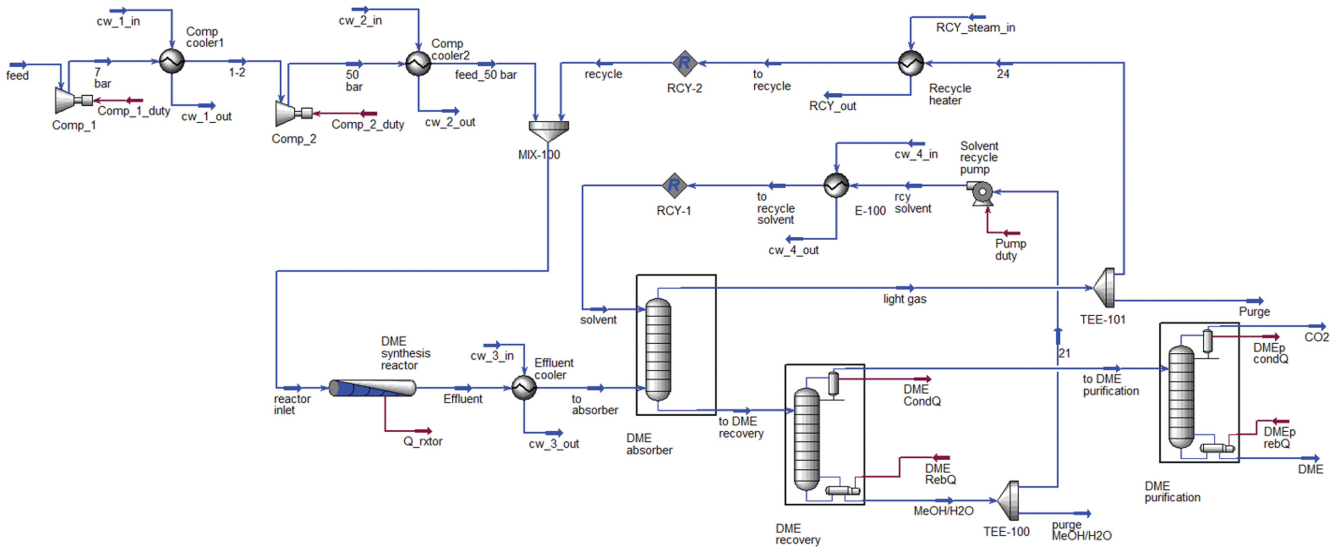

Fig. S7. Process scheme of Case 2-R1.

Table S6. Heat and mass balance for Case 2-R1

Name	Feed	Reactor inlet	Effluent	Light gas	to DME recovery	to DME purification	Solvent	Purge MeOH/H_2O	CO_2	DME
Temperature [C]	25.00	249.97	207.71	25.28	27.93	39.79	25.00	166.15	9.97	42.87
Pressure [kPa]	101.32	5,000.00	5,000.00	5,000.00	5,000.00	1,000.00	5,000.00	1,000.00	1,000.00	1,000.00
Molar flow [kgmol/h]	8,581.69	47,798.83	45,359.64	43,515.82	34,849.40	611.25	33,005.59	1,232.91	120.03	491.22
Mass flow [kg/h]	115,000.00	706,254.11	706,273.95	655,459.00	700,594.64	26,548.49	649,779.69	24,272.25	3,950.46	22,598.03
H_2 [kg/h]	8,823.38	34,092.16	28,061.22	28,035.42	25.80	25.80	0.00	0.00	25.80	0.00
CH_4 [kg/h]	30,288.48	299,698.37	299,698.37	299,297.73	400.64	400.64	0.00	0.00	391.70	8.94
CO [kg/h]	19,230.29	23,446.35	4,734.84	4,695.45	39.40	39.40	0.00	0.00	39.40	0.00
N_2 [kg/h]	26,443.82	262,386.72	262,386.72	262,061.25	325.47	325.47	0.00	0.00	325.37	0.10
CO_2 [kg/h]	30,214.03	83,333.11	59,054.13	57,967.04	1,087.09	1,087.09	0.00	0.00	1,009.72	77.37
DME [kg/h]	0.00	749.84	25,573.54	905.17	25,317.83	24,643.51	649.46	24.28	2,158.47	22,485.04
MeOH [kg/h]	0.00	1,970.29	6,542.21	1,840.77	129,849.29	26.55	125,147.86	4,674.89	0.00	26.55
H_2O [kg/h]	0.00	577.27	20,222.91	656.17	543,549.11	0.03	523,982.37	19,573.08	0.00	0.03

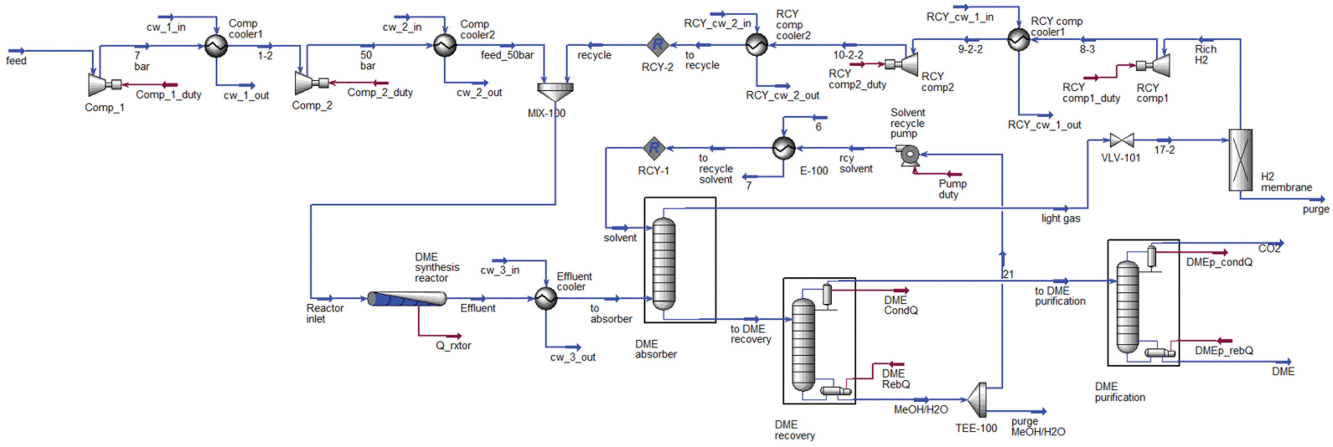

Fig. S8. Process scheme of Case 2-R2.

Table S7. Heat and mass balance for Case 2-R2

Name	Feed	Reactor inlet	Effluent	Light gas	to DME recovery	Solvent	Purge MeOH/H_2O	to DME purification	CO_2	DME	Purge	Recycle
Temperature [C]	25.00	249.82	217.70	26.00	32.75	25.00	163.38	42.69	10.00	42.62	23.82	250
Pressure [kPa]	101.32	5,000.00	5,000.00	5,000.00	5,000.00	5,000.00	1,000.00	1,000.00	1,000.00	1,000.00	910.00	5,000
Molar flow [kgmol/h]	8,581.69	15,550.65	13,278.64	11,645.42	9,202.83	7,569.62	1,137.25	495.61	47.10	448.50	4,672.37	6,968.962
Mass flow [kg/h]	115,000.00	155,963.59	155,964.15	110,795.31	197,875.43	152,706.59	22,942.28	22,219.96	1,579.94	20,640.02	69,793.37	40,963.59
H_2 [kg/h]	8,823.38	21,268.70	15,681.89	15,663.05	18.83	0.00	0.00	18.83	18.74	0.09	3,210.93	12,445.33
CH_4 [kg/h]	30,288.48	33,241.14	33,241.14	33,175.55	65.59	0.00	0.00	65.59	62.07	3.52	30,222.93	2,952.664
CO [kg/h]	19,230.29	19,402.02	1,564.42	1,549.61	14.81	0.00	0.00	14.81	14.70	0.11	1,377.60	171.7326
N_2 [kg/h]	26,443.82	28,640.22	28,640.22	28,598.52	41.70	0.00	0.00	41.70	41.13	0.57	26,402.15	2,196.399
CO_2 [kg/h]	30,214.03	53,411.50	31,442.82	30,766.65	676.17	0.00	0.00	676.17	605.70	70.47	7,537.83	23,197.46
DME [kg/h]	0.00	0.00	21,774.09	370.47	21,556.32	152.70	22.95	21,380.61	837.59	20,543.01	370.47	0
MeOH [kg/h]	0.00	0.00	6,112.06	514.49	42,709.35	37,111.79	5,575.35	22.22	0.00	22.22	514.49	0
H_2O [kg/h]	0.00	0.00	17,507.51	156.97	132,792.64	115,442.10	17,343.98	0.02	0.00	0.02	156.97	0

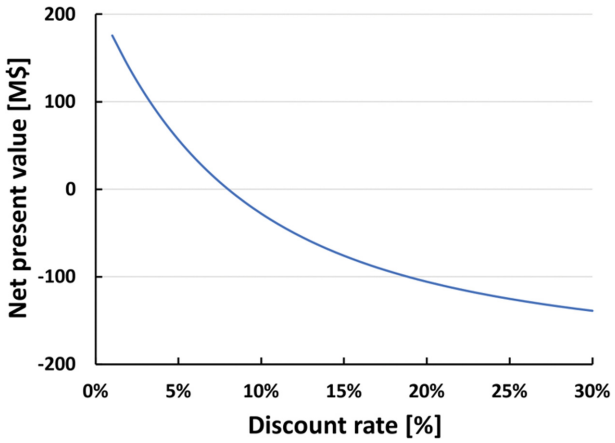

Fig. S9. NPV profile of Case 2-R2.